Cell

Architecture-Dependent Noise Discriminates Functionally Analogous Differentiation Circuits

Tolga Çağatay,[1,2] Marc Turcotte,[2] Michael B. Elowitz,[3] Jordi Garcia-Ojalvo,[4] and Gürol M. Süel[1,2,*]
[1]Green Center for Systems Biology
[2]Department of Pharmacology
University of Texas Southwestern Medical Center, Dallas, TX 75390, USA
[3]Division of Biology and Department of Applied Physics, California Institute of Technology, Pasadena, CA 91125, USA
[4]Departament de Física i Enginyeria Nuclear, Universitat Politècnica de Catalunya, Colom 11, E-08222 Terrassa, Spain
*Correspondence: gurol.suel@utsouthwestern.edu
DOI 10.1016/j.cell.2009.07.046

SUMMARY

Gene regulatory circuits with different architectures (patterns of regulatory interactions) can generate similar dynamics. This raises the question of why a particular circuit architecture is selected to implement a given cellular process. To investigate this problem, we compared the *Bacillus subtilis* circuit that regulates differentiation into the competence state to an engineered circuit with an alternative architecture (SynEx) in silico and in vivo. Time-lapse microscopy measurements showed that SynEx cells generated competence dynamics similar to native cells and reconstituted the physiology of differentiation. However, architectural differences between the circuits altered the dynamic distribution of stochastic fluctuations (noise) during circuit operation. This distinction in noise causes functional differences between the circuits by selectively controlling the timing of competence episodes and response of the system to various DNA concentrations. These results reveal a tradeoff between temporal precision and physiological response range that is controlled by distinct noise characteristics of alternative circuit architectures.

INTRODUCTION

A fundamental problem in biology is explaining what constraints have selected for observed architectures (i.e., topologies) of gene regulatory circuits. Recently, genetic circuits with different connectivity maps have been shown to generate similar dynamics and function (Alon, 2007; Kollmann et al., 2005; Mangan and Alon, 2003; Stricker et al., 2008; Tsai et al., 2008). This raises the important question as to why particular circuit topologies are present in cells when the same function can supposedly be obtained from alternative architectures. Experimental investigation of this problem is challenging because biological circuits are typically comprised of many components, some unknown, and

control physiological processes that are not fully understood, complex in behavior, and difficult to measure quantitatively. Differentiation of *B. subtilis* cells into the competence state represents an ideal model system to study this problem because the underlying genetic circuit and its biological function are relatively simple and well characterized (Dubnau, 1999; Grossman, 1995). Additionally, standard tools for genetic manipulation of *B. subtilis* permit the construction of alternative genetic circuits to probe the functional importance of the native competence circuit architecture.

Under environmental stress, a small fraction of *B. subtilis* cells transiently differentiate into the state of competence, in which they are capable of taking up extracellular DNA and incorporating it into their chromosome (Dubnau, 1999; Grossman, 1995). Differentiation into competence is regulated by a relatively simple core circuit (Figure 1A). At the heart of the circuit is the transcription factor ComK, which is necessary and sufficient to trigger competence and controls the expression of over 140 genes (Berka et al., 2002; van Sinderen et al., 1995). ComK activates its own expression, forming a positive feedback loop (Maamar and Dubnau, 2005; Smits et al., 2005). Exit from competence occurs via a negative feedback loop in which ComK indirectly represses the expression of its activator ComS (Hahn et al., 1994; Smits et al., 2007; Süel et al., 2006). Cell-cell communication under environmental stress conditions induces expression of ComS, which in turn favors build up of ComK concentration by competitively interfering with the proteolytic degradation of ComK (Magnuson et al., 1994; Ogura et al., 1999; Turgay et al., 1998). Repression of ComS expression during competence increases ComK degradation and thus permits exit from competence (Smits et al., 2007; Süel et al., 2006, 2007). Together, the interacting positive and negative feedback loops constitute a noise-driven excitable system, which in response to small threshold-crossing perturbations generates a large-amplitude transient response (Figure 1B) (Maamar et al., 2007; Süel et al., 2006; Süel et al., 2007).

A crucial aspect of competence is the negative feedback loop in which ComK indirectly stimulates its own degradation, permitting cells to exit the competent state (Ogura et al., 1999; Turgay et al., 1998). The architecture of this negative feedback loop is
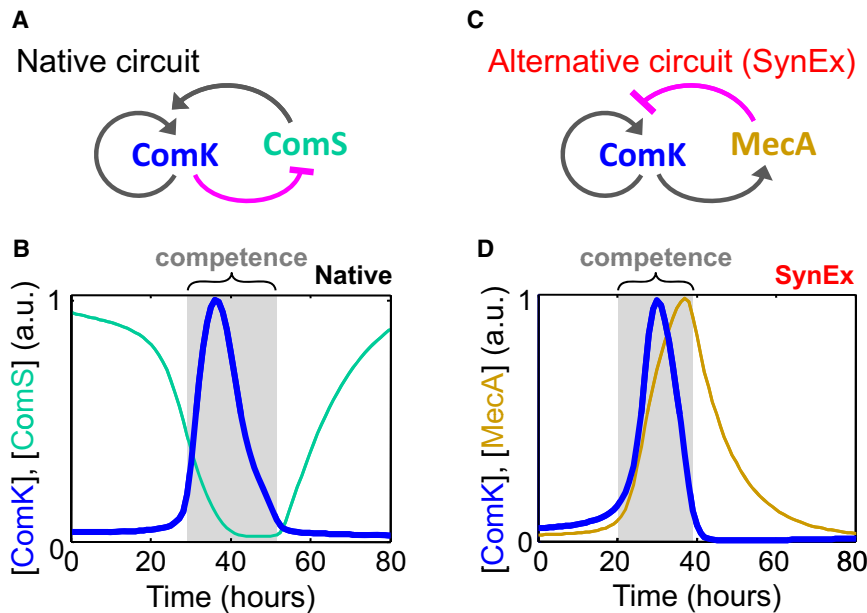
Cell

Figure 1. An Alternative Gene Circuit Architecture, SynEx, Is Predicted to Generate Competence Dynamics Equivalent to the Native Circuit

(A) Simplified diagram of the native *B. subtilis* competence circuit. The competence master regulator ComK positively autoregulates its own expression, forming a positive feedback loop. ComK also represses ComS, which in turn promotes high ComK concentrations consequently establishing a net negative feedback loop.

(B) Deterministic simulations of the native *B. subtilis* competence circuit. A transient pulse of ComK (blue) activity corresponds to competence (gray area). During competence, ComS (green) expression is negatively correlated with ComK.

(C) Diagram of the alternative SynEx circuit architecture. SynEx shares the ComK positive feedback loop with the native circuit, but varies in the topology of the net negative feedback loop. ComK induces expression of MecA, which induces degradation of ComK. Thus, in the SynEx circuit the reactions comprising the net negative feedback loop are interchanged with respect to the native circuit.

(D) Deterministic simulations of the SynEx circuit generate a transient pulse of ComK (blue) corresponding to competence (gray area) that is equivalent to the native circuit. In the SynEx circuit, MecA (yellow) concentration is positively correlated with ComK during competence.

not the only one that supports excitable dynamics. Genetic oscillators such as the circadian clock are based on genetic circuits that differ in topology, but are also capable of generating excitable dynamics (Turcotte et al., 2008). This raises two general questions: First, what design tradeoffs exist between alternative excitable circuit architectures? Second, what other capabilities besides excitability, per se, does the native architecture provide to the system?

In order to address these questions, we constructed a physiologically functional synthetic differentiation circuit (SynEx) with an alternative architecture (Figure 1C). This allowed us to systematically compare competence circuits with different topologies in vivo. Mathematical modeling and quantitative measurements at the single-cell level of the native and synthetic circuits revealed that the architecture of the native competence circuit generates higher variability in the duration of competence episodes. This variability in circuit dynamics at the cellular level determines the range of environmental conditions at the population level to which the competence system can respond. These results suggest that environmental constraints can select for specific architectures of gene regulatory circuits, based on noise in circuit dynamics.

RESULTS

Construction of an Alternative Competence Circuit Architecture

An alternative to the native competence circuit was designed by interchanging the inhibitory and activating interactions comprising the negative feedback loop (compare Figures 1A and

1C). Whereas in the native circuit, ComK represses its activator ComS, in the alternative SynEx circuit, ComK induces expression of the protein responsible for its degradation, MecA. Therefore, exit from competence in SynEx is achieved by expression of the inhibitor MecA, rather than repression of the activator ComS. The SynEx negative feedback loop topology, where a repressor is activated, is also a shared feature of genetic oscillators (see Figure S17 available online). In order to compare the potential behaviors of the native and SynEx circuits, we first constructed differential equation models of both circuits (see the Supplemental Experimental Procedures [S1.1.1, S1.2.1]). These models serve as frameworks for data analysis and tools for hypothesis generation. A critical advantage is that the ComK positive feedback loop is identical between the native and SynEx circuits, allowing specific comparison between the two negative feedback architectures. Simulations showed that similar to the native circuit, SynEx can also access a regime of excitable dynamics. Therefore, both circuits are predicted to generate transient pulses of ComK with similar frequency, duration and amplitude (Figures 1B and 1D). Due to the different negative feedback loop architectures, ComS concentration in the native circuit is negatively correlated with ComK concentration, while MecA in the SynEx circuit is positively correlated with ComK (Figures 1B and 1D). Despite this difference in correlations, the dynamics of ComK in the native and SynEx circuits are similar in continuous simulations.

To test these predictions in vivo, we constructed the SynEx circuit in *B. subtilis* and compared its behavior with that of the native circuit. We first deleted the native ComS-mediated negative feedback loop by knocking out the *comS* gene. An
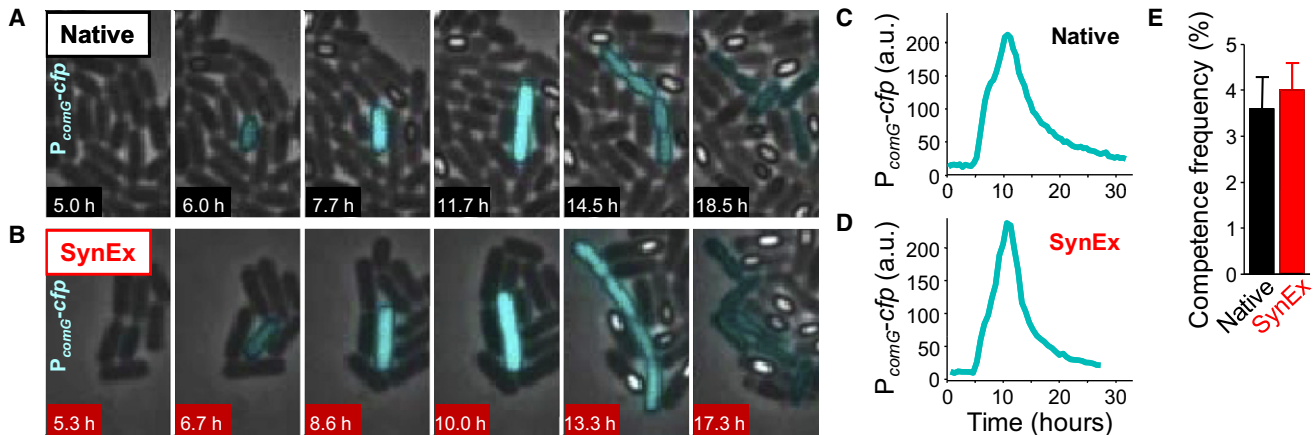
Figure 2. The Engineered SynEx Circuit Generates Native-like Single-Cell Competence Dynamics and Reconstitutes Physiological Function In Vivo

(A and B) Filmstrips of native and SynEx cells respectively, undergoing a transient episode of competence. For both strains, shown are overlays of phase contrast and P_{comG}-*cfp* fluorescence (in cyan), a reporter for competence. Times in hours are indicated in each frame.

(C and D) Quantitative P_{comG}-*cfp* time traces of native and SynEx competence events respectively obtained from corresponding cells shown in (A) and (B).

(E) Mean percent frequency of competence in the native and SynEx strains. Error bars indicate standard error of the mean (SEM).

isopropyl-β-D-thiogalactopyranoside (IPTG) inducible promoter expressing ComS was then introduced chromosomally to control the probability of competence events (Quisel et al., 2001). Expression of ComS in these cells was therefore no longer influenced by ComK dynamics (see Figure S10). As expected in this strain without the native ComS-mediated negative feedback loop, cells that entered competence were unable to exit (see the Supplemental Experimental Procedures [S2.8]). Next, we introduced the alternative SynEx negative feedback loop. We placed the *mecA* gene under the control of the ComK-specific *comG* promoter (P_{comG}) and inserted this construct into the *B. subtilis* chromosome (Hamoen et al., 1998). During competence, high concentrations of ComK result in transcriptional activation of MecA, which in turn targets ComK for degradation, permitting cells to exit competence. Mathematical modeling was utilized as a guide to tune and optimize the SynEx circuit in vivo. For example, simulations showed that high affinity of the P_{comG} promoter for binding ComK would prevent excitable dynamics, because expression of P_{comG}-*mecA* at low ComK concentrations would inhibit activation of the ComK positive feedback loop and thus preclude competence. Consistent with these theoretical results, we observed competence in vivo only after introducing a point mutation in the P_{comG} promoter that reduced affinity for ComK binding (Susanna et al., 2007) (see the Supplemental Experimental Procedures [S2.4]).

Engineered SynEx Circuit Reconstitutes Single-Cell Dynamics and Frequency of Competence In Vivo

We experimentally tested the ability of the engineered SynEx circuit to generate excitable competence dynamics and functionally substitute for the native circuit. Accordingly, we measured native and SynEx circuit dynamics at the single-cell level through quantitative fluorescence time-lapse microscopy (Figures 2A and 2B). Select sample pulses of the competence reporter P_{comG}-*cfp* activity observed in SynEx cells appeared

to be similar in shape and amplitude to those seen in native cells (Figures 2C and 2D). To enable direct comparison, we tuned the SynEx circuit (see the Supplemental Experimental Procedures [S2.4]) to have the same frequency of cells that access the competence state (defined by P_{comG}-*cfp* reporter activity) as the natural system (4% ± 0.6% in SynEx and 3.6% ± 0.7% in native cells) (Figure 2E). These results indicate that, as predicted mathematically, the SynEx circuit generates excitable dynamics with similar shape and frequency compared to the native competence circuit.

Differences between SynEx and Native Competence Events

Despite similarities in the single-cell dynamics of native and SynEx circuits, the two strains also displayed several differences. First, the cell-cell variability of competence durations was distinct between native and SynEx (Figure 3A). Specifically, the distribution of duration times of the native circuit was broader than that of the SynEx circuit (Figure 3B). Therefore, the SynEx circuit was twice as precise compared to native with coefficients of variation (noise) of 0.26 (n = 77) and 0.51 (n = 91), respectively (Figure 3C). Second, the median duration of competence events differed between the two circuits (Figure 3D). Native competence events lasted approximately twice as long as their SynEx counterparts (15 hr versus 7 hr, respectively). Third, while SynEx cells were able to reconstitute the physiological function of competence, they did so with a reduced efficiency (Figure 3E). Transformation assays showed that native cells had a 6-fold higher efficiency than cells with the SynEx circuit in taking up extracellular DNA and incorporating it into their chromosome. These results provoke the following questions regarding the observed differences between the two circuits: First, what about the circuits accounts for the difference in cell-cell variability between native and SynEx competence durations? Second, are shorter SynEx competence events responsible for the reduced transformation
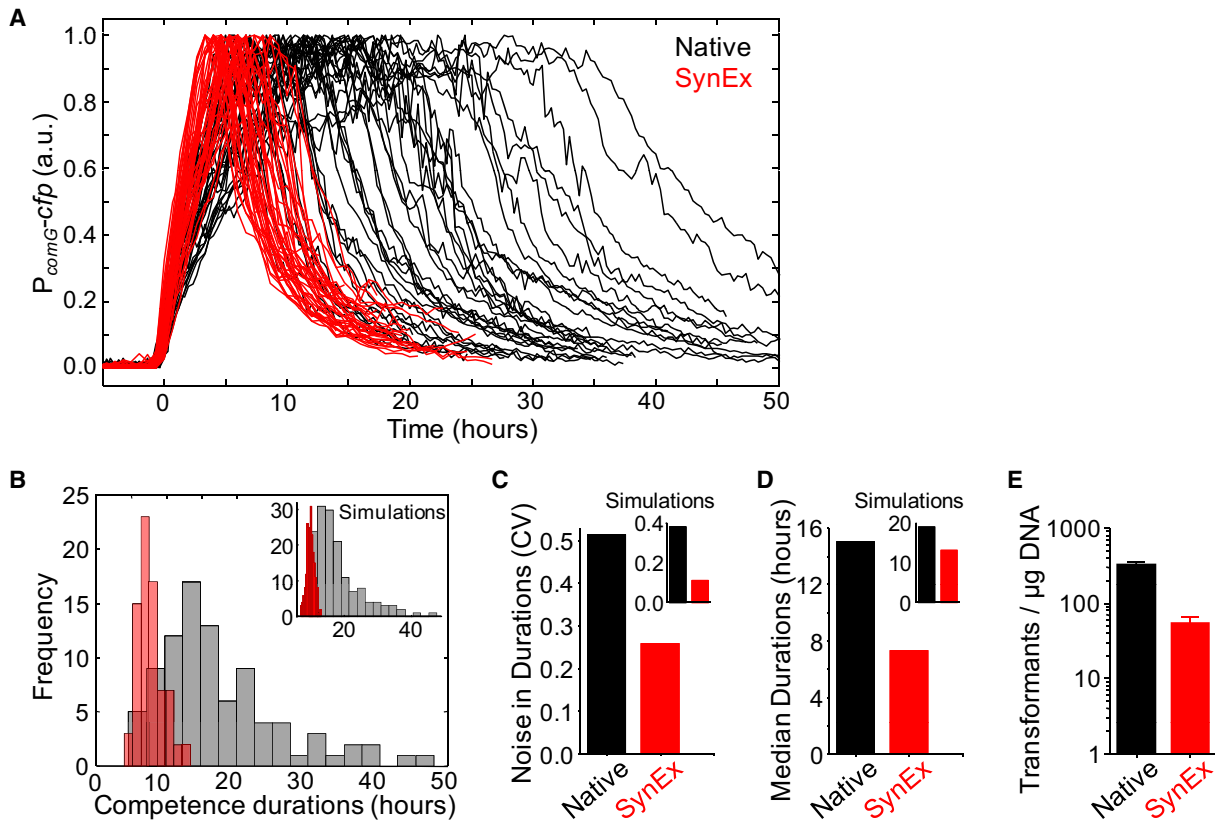
Cell

Figure 3. SynEx Circuit Competence Duration Times Are More Precise than Those of Its Native Counterpart at the Single-Cell Level

(A) Sample time traces of competence episodes as measured by P$_{comG}$-*cfp* fluorescence activity for native (black) and SynEx (red) cells. All time traces have been normalized for amplitude and aligned with respect to initiation of competence to aid visual comparison.

(B) Histograms of all native (n = 91) and SynEx (n = 77) competence durations.

(C) Coefficient of variation (noise) of competence duration times shown in (B) for native and SynEx cells as indicated.

(D) Median duration times of native and SynEx competence events shown in (B).

(B, C, and D) Insets show corresponding results obtained from discrete stochastic simulations of the native and SynEx circuits.

(E) Mean number of transformants of native and SynEx cells transformed with 2 μg extracellular DNA. Color-coded error bars indicate the SEM. The number of transformants is a measure of the efficiency of physiological function of competence for both native and SynEx strains.

efficiency? Third, does the variability of competence durations play a functional role? We systematically investigated these differences to obtain insight into the relationship between competence circuit architecture, dynamics and function.

Low Molecule Numbers of ComS Are the Source of Variability in Native Competence Durations

To identify the source of the difference in precision between the SynEx and native circuit dynamics, we constructed discrete stochastic models of the native and SynEx circuits to account for intrinsic noise of biochemical reactions and simulated them using the Gillespie algorithm (Gillespie, 1977) (see the Supplemental Experimental Procedures [S1.1.2 and S.1.2.3]). In both the native and SynEx circuits, the concentration of ComK during competence events is similarly high and therefore does not contribute to differences in stochastic fluctuations between the two circuits (Figures 4A and 4B). However, ComS expression during competence in the native circuit is repressed, and its concentration drops to a few molecules per cell, thus becoming subject to high-amplitude stochastic fluctuations relative to its

mean concentration (Figure 4A). In contrast, the concentration of MecA in the SynEx circuit is positively correlated with ComK and thus remains high and relatively less subject to noise during competence (Figure 4B). These stochastic simulations suggest that the opposite regulatory modes of repressing an activator (ComS) versus activating an inhibitor (MecA) contributed to the variation in precision between the native and SynEx circuits, respectively.

To further study the noise behavior of native and SynEx circuits, we numerically tested perturbations to biochemical parameters designed to alter the level of fluctuations in ComS and MecA, respectively. For example, to reduce noise in ComS and MecA, we increased expression rates of their respective promoters and compensated for this difference by lowering their binding affinities by a similar fold change. We refer to this combination of compensating parameter changes as the "noise scaling factor" (Figure 4C). Together, these perturbations increased the molecule numbers of ComS and MecA without changing their mean activity and dynamics. Variability in competence durations of native and SynEx circuits was observed to
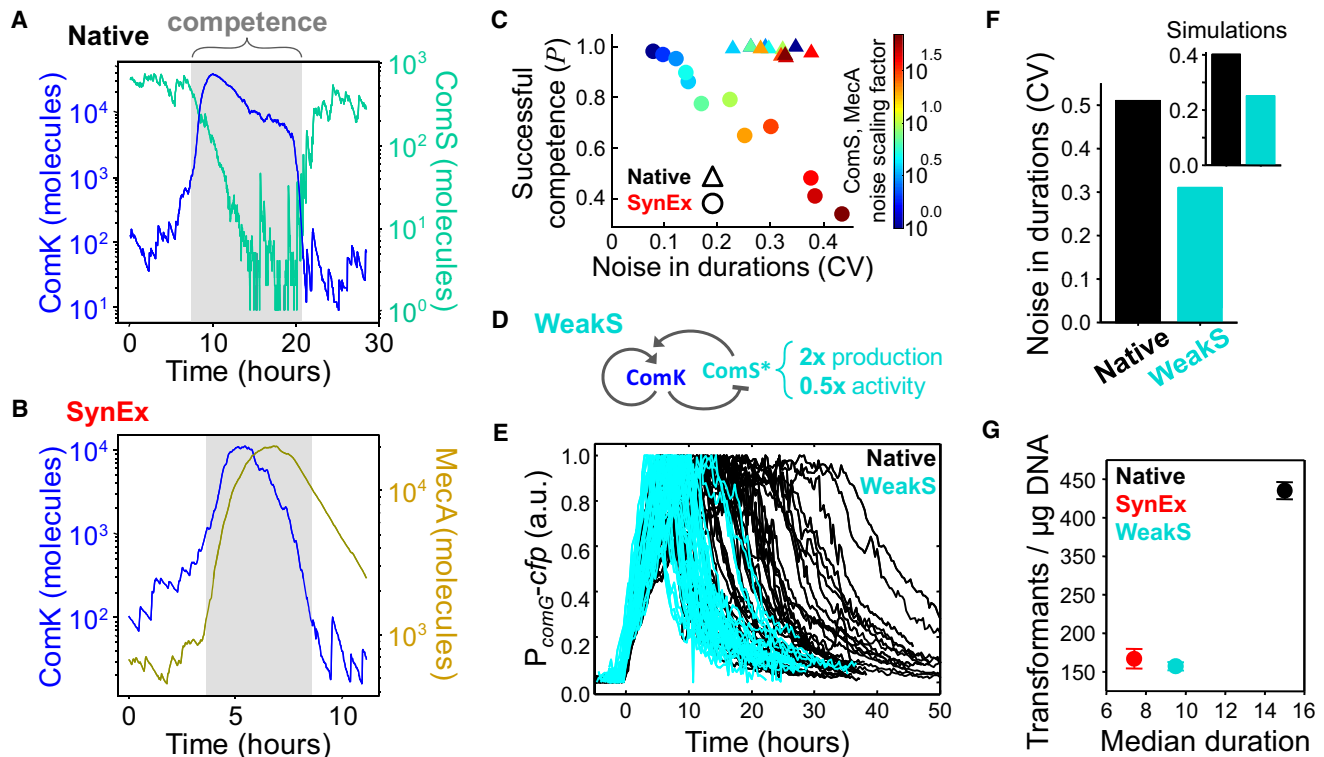
Figure 4. Comparison of Native and SynEx Circuits Identifies the Source of Variability in Competence Duration Times

(A) Sample time traces of discrete stochastic simulations of the native circuit depicting ComK (blue) and ComS (green) molecule numbers during competence (gray area). Note the low molecule number and high amplitude stochastic fluctuations in ComS during competence.

(B) Sample time traces of discrete stochastic simulations of the SynEx circuit depicting ComK (blue) and MecA (yellow) molecule numbers. Note that time traces of ComK are comparable between native and SynEx circuits; however, molecule numbers of respective negative feedback loop components ComS and MecA are oppositely correlated.

(C) Probability of successful native and SynEx competence events as defined by sufficiently high ComK amplitude is shown as a function of variability in competence durations. Note that this is different from the frequency of competence which is a measure of the fraction of competent cells in a population. Color coding of data points refers to the "noise scaling factor" (described in the main text) that controls the ComS and MecA promoter expression rates and binding affinities, which were adjusted in a compensatory manner to scale the relative fluctuations in molecule numbers during competence (see also the Supplemental Experimental Procedures [S1.3]). Color coding of data points from blue to red indicate increasing noise scaling factor, which corresponds to increasing fluctuations in ComS or MecA molecule numbers in native and SynEx models, respectively.

(D) Cartoon describing the experimental perturbations to ComS parameters that together comprise the WeakS strain. ComS* denotes that the native *comS* gene has been replaced by two copies of a mutated version that has half the affinity to the protease complex that targets ComK for degradation (see also the main text).

(E) Sample time traces of experimental competence episodes as measured by P$_{comG}$-*cfp* fluorescence activity for native (black) and WeakS (cyan) cells. All time traces have been normalized for amplitude and aligned with respect to initiation of competence to aid visual comparison.

(F) Variability in competence durations as measured by CV obtained from experimental measurements of the data shown in (E) and simulations described in the main text (see also the Supplemental Experimental Procedures [S1.3]).

(G) Correlation between absolute transformation efficiencies of native, SynEx, and WeakS strains and their respective median competence duration times. Transformations were performed in triplicates and in parallel using 1 μg of the same plasmid to permit direct comparison between the strains.

depend on fluctuations in ComS and MecA concentrations, respectively, which could be controlled by the noise scaling factor (see color coding of data points in Figure 4C). However, the two circuits exhibited distinct trends in terms of peak ComK amplitudes, defined here as the probability, *P*, for generating successful competence events (Figure 4C). Specifically, in the SynEx circuit, increased variability in competence duration comes at the cost of a much higher variability in ComK pulse amplitudes than in the native circuit (see the Supplemental Experimental Procedures [S1.3] and Figure S7). Such variability in amplitude interferes with the ability of ComK to cross the putative competence threshold in a reliable manner. Consequently,

the probability *P* of the SynEx circuit to generate successful competence events is reduced with increasing variability of competence durations (Figure 4C). In contrast, in the native circuit *P* is less sensitive to changes in duration noise (Figure 4C). Therefore, the SynEx circuit seems to be unable to generate high variability in competence durations without loss of competence function, in contrast to the native circuit. Similarly, a more general global parameter analysis showed that random variation of all parameters of the native and SynEx circuits also generates distinct noise profiles for each circuit architecture (see the Supplemental Experimental Procedures [S1.4]).

Cell

Next, we experimentally tested the hypothesis that low molecule numbers of ComS during native competence events give rise to variability in durations. To that end, we constructed a WeakS strain in which we introduced two compensating perturbations to ComS, corresponding to those described in the preceding paragraph, such that twice the number of ComS molecules was required to maintain its mean cellular activity (Figure 4D). Specifically, native ComS was replaced with two copies of a mutated version of ComS shown to have 50% reduced affinity to the proteolytic degradation complex that targets ComK (Ogura et al., 1999). The number of ComS molecules during WeakS competence events was therefore expected to be twice as high compared to native cells. Consequently, variability in WeakS competence duration times was predicted theoretically to be lower than native (Figure 4F, inset). We measured competence dynamics in WeakS cells and observed that noise in competence durations was indeed reduced by 39% (coefficient of variation [CV] = 0.31, n = 40) compared to native (Figures 4E and 4F). Similarly, a strain in which both copy number and degradation of ComS were increased (HighS) exhibited a 25% reduction (CV = 0.39, n = 38) in the variability of competence durations (see SOM S2.6). These data are consistent with simulations and together suggest that high ComS noise during competence, due to low molecule numbers, is the main source of variability in competence durations for native cells.

SynExSlow Reveals Relationship between Mean Competence Durations and Absolute Transformation Efficiency

Both SynEx and WeakS strains exhibited shorter mean duration times and reduced transformation efficiency compared to native (Figure 4G). These data suggested that mean duration times of competence may determine the absolute efficiency of DNA uptake during competence. However, although the frequency of competence events in the SynEx circuit was similar to native, it was lower in the WeakS strain (0.5% ± 0.2%, compared to 4% ± 0.6% in SynEx and 3.6% ± 0.7% in native). This difference hindered a direct test of the relationship between mean competence durations and absolute transformation efficiency. Therefore, to experimentally investigate the relationship between mean competence durations and transformation efficiency, we constructed an additional *B. subtilis* strain (SynExSlow) similar in topology to SynEx but capable of generating mean competence durations equivalent to native cells (Figure 5A). We engineered the SynExSlow strain by modifying the SynEx circuit to generate longer mean competence duration times in accordance with predictions from simulations (Figure 5B). In particular, we reduced the efficiency of the MecA-mediated negative feedback loop to delay exit from competence. This was accomplished by competitively interfering with the proteolytic degradation of ComK by MecA during competence and thus extending competence durations (Figures 5C and 5D, and see the Supplemental Experimental Procedures [S2.7]). A comparative analysis of native, SynEx, and SynExSlow strains could therefore distinguish the physiological advantages of longer mean competence durations observed in native cells.

The SynExSlow strain produced mean competence durations and absolute transformation efficiency equivalent to native. As

anticipated, SynExSlow competence events occurred at a frequency (3.2% ± 0.4%) that was similar to SynEx and native strains (Figure 5E). In contrast to SynEx, however, the median duration of SynExSlow competence events was similar to native (Figure 5F). The transformation efficiency of the SynExSlow strain was also similar to native for extracellular DNA concentrations ≥1 μg/ml (Figure 5G). These results suggested that longer mean durations of competence events increase the absolute efficiency of transformations, thus explaining the lower transformation efficiency of the SynEx strain.

Despite similar mean competence durations and transformation efficiency, SynExSlow cells differed from their native counterparts in the variability of competence durations (Figure 5H). SynExSlow competence durations did not include very short or long episodes observed in native cells and thus exhibited less noise in competence durations (CV = 0.27, n = 65) (Figures 5C and 5D). Although SynEx and SynExSlow strains have distinct transformation efficiency and mean competence durations, both circuits displayed similar noise in competence durations (0.26 and 0.27, respectively) (Figure 5H). These results show that competence circuits that share the SynEx negative feedback loop architecture also display similar low noise in durations even if they differ in other competence properties. The SynExSlow strain was therefore equivalent to native in all properties except for variability in competence durations and thus provided the opportunity to exclusively investigate the functional importance of noise in competence durations.

Noise in Competence Durations Facilitates Response to Variable Environments

We investigated whether higher noise in native competence durations provides a functional advantage that is distinct from that of longer mean durations. The biological function of competence is to take up and incorporate extracellular DNA into the chromosome of *B. subtilis* cells (Dubnau, 1999) One possible model to predict the probability of DNA uptake (transformation efficiency) is based on comparing two characteristic times: (1) the diffusion time for cells to encounter DNA in the extracellular medium, which is inversely proportional to extracellular DNA concentration, and (2) the duration of competence (see the Supplemental Experimental Procedures [S1.6]). Longer durations of competence can increase the probability of DNA uptake, but may be deleterious since competent cells have been experimentally shown to exhibit a reduced growth rate (Haijema et al., 2001; Süel et al., 2006). Given unpredictability in extracellular DNA concentrations, optimization of this cost-benefit problem may give rise to variability in competence duration times (Acar et al., 2008; Blake et al., 2006; Kussell and Leibler, 2005; Thattai and van Oudenaarden, 2004; Wolf et al., 2005). Therefore, while longer mean durations contribute to absolute transformation efficiency, higher variability in durations is expected to facilitate efficient response to a wide range of extracellular DNA concentrations.

To test this prediction, we measured the dependence of transformation efficiency on extracellular DNA concentration using transformation assays based on counting the number of transformants at different DNA concentrations (Figure 6A). The SynEx and SynExSlow populations displayed a relatively large
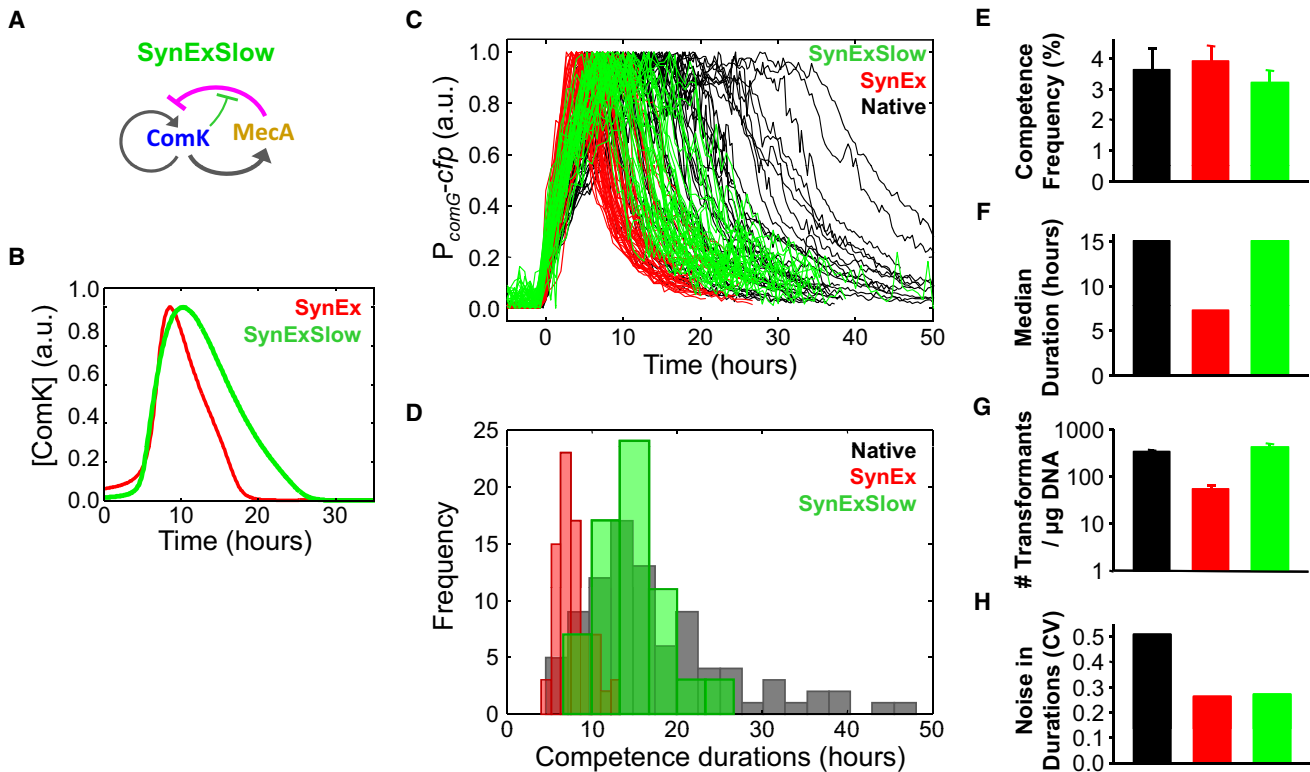
Cell

Figure 5. SynExSlow Differs from the Native Circuit Only in Noise of Competence Durations

(A) Cartoon depicting the SynExSlow strain.

(B) Continuous simulation ComK time traces of SynEx and SynExSlow circuits (see the Supplemental Experimental Procedures [S1.5]). The SynExSlow strain is predicted to generate longer competence events.

(C) Sample time traces of competence episodes as measured by P_{comG}-cfp fluorescence activity for native (black), SynEx (red), and SynExSlow (green) cells. All time traces have been normalized for amplitude and aligned with respect to initiation of competence to aid visual comparison.

(D) Histograms of competence duration times for native (gray; n = 91), SynEx (red; n = 77), and SynExSlow (green; n = 65).

(E–H) Colors of bar graphs shown depict native (black), SynEx (red), and SynExSlow (green).

(E) Mean frequency of competence events. Error bars indicate the SEM.

(F) Median durations of competence events obtained from the histograms shown in (D).

(G) Mean number of transformants obtained with transformations using identical 2 μg extracellular plasmid for all strains. Error bars the indicate SEM.

(H) CV of competence duration times.

difference in normalized transformation efficiencies over a 50-fold range in DNA concentrations. However, over the same range in DNA concentrations, normalized transformation efficiencies of the native population exhibited a relatively small change. The flatter response curve of the native strain indicated that efficiency of DNA uptake is maintained despite differences in extracellular DNA concentration, suggesting that native cells are better equipped to cope with variable environmental conditions.

To quantify the change in transformation efficiency as a function of DNA concentration, we fit the data to a simple sigmoidal Hill function dose-response curve (Figure 6A). The Hill coefficient of the sigmoid reports how sharply the relative transformation efficiency changes as a function of extracellular DNA concentration, and was calculated to be 0.7, 1.2, and 1.4 for native, SynExSlow, and SynEx populations, respectively (Figure 6A). The disparity in sensitivity reported by Hill coefficients was remarkably reproducible even with variation in the absolute

numbers of more than 58,000 total colonies counted in a minimum of seven independent experiments for each strain. The nearly 2-fold difference in Hill coefficients among the native and synthetic circuits shows that SynEx and SynExSlow transformations are more sensitive, and thus display a narrower response range, with respect to differences in extracellular DNA concentrations. These results correlate with the similar level of noise in competence duration times exhibited by the synthetic circuits (Figure 6B). Together, these data show that noise in competence circuit dynamics can determine the range of environmental conditions, i.e., DNA concentrations, in which the system can function effectively.

These results imply that the physiological function of competence at the population-level of native and SynEx strains depends on competence circuit dynamics at the single-cell level. A simple model of the transformation process (see the Supplemental Experimental Procedures [S1.6]) indicates that the sigmoidal dose response curves shown in Figure 6A can be

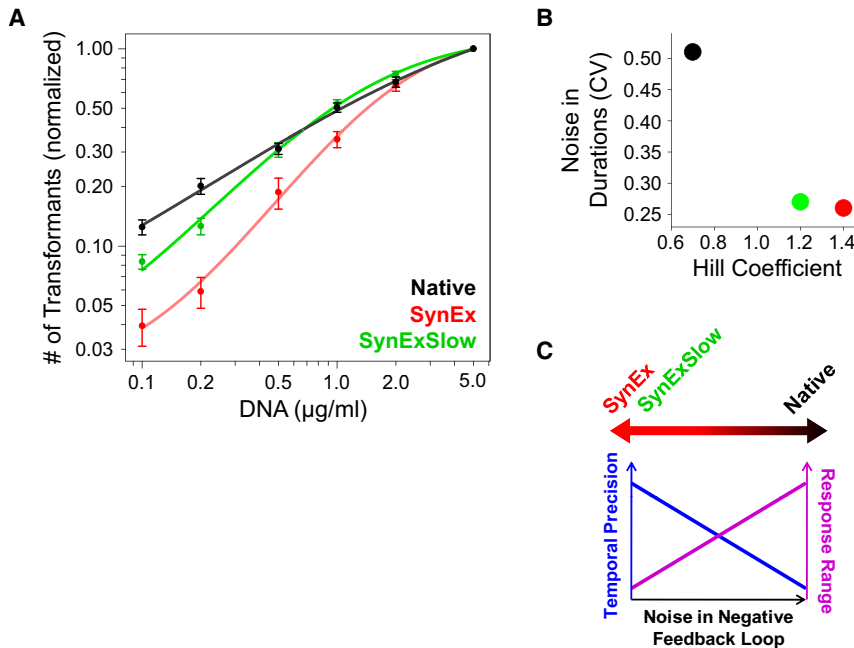**Cell**

A

B

C

Figure 6. Noise in Competence Duration Times in Native Cells Increases Robustness of Competence Physiology under Varying Extracellular DNA Concentrations

(A) Doubly logarithmic plot of the number of transformants normalized to the same maximum value, as a function of DNA concentrations. Normalization permits direct visual comparison of relative change in transformation efficiency as a function of extracellular DNA concentrations among the strains. Data points depict mean and SEM of a minimum of seven independent experiments with a total of 58,000 colonies counted for native (black), SynEx (red), and SynExSlow (green) strains. To permit direct comparison, all strains were transformed with the same plasmid. Solid lines represent fits of the data to a standard sigmoidal Hill function. The Hill coefficients of the respective dose response curves are 0.7 for native, 1.2 for SynExSlow, and 1.4 for SynEx circuits.

(B) Correlation plot of noise (coefficient of variation) in competence durations versus Hill coefficient obtained from transformation response curves for native (black), SynEx (red), and SynExSlow (green) strains. Higher noise in competence duration times is negatively correlated with Hill coefficient.

(C) Cartoon depicting the tradeoff between temporal precision of single-cell dynamics and response range at the population level that appears to be regulated by noise in the negative feedback loop regulator of the respective circuits indicated above.

accounted for from the cumulative integrals of the distributions of competence durations plotted in Figure 3B. According to the model, the location of the inflection point of the transformation response curve is influenced by the mean of the underlying distribution of competence durations. Consistent with this prediction, the location of the SynExSlow transformation response curve was closer to native than SynEx, in accordance with their respective median competence durations (Native = 15.0 hr, SynExSlow = 14.7 hr, and SynEx = 7.4 hr). In contrast, the slope at the inflection point of the transformation response curve is predicted to be controlled by the variability (noise) in the distribution of competence durations. Similar steepness of SynEx and SynExSlow transformation response curves is thus consistent with their comparable variability in competence durations (CV = 0.26 and CV = 0.27, respectively). Therefore, it is noise in competence duration times, and not the mean duration or absolute transformation efficiency of competence events, that determines the relative response range of competence.

DISCUSSION

It is difficult to predict cellular and physiological behavior from molecular interactions that comprise underlying gene regulatory circuits. For example, there may not be a simple relationship that describes how the dynamics of molecular processes contribute to the amplitude or range of cellular responses. However, we find here that measurement of variability in gene circuit dynamics at the single-cell level permits prediction of the physiological response range at the population level. In particular, noise in

native competence durations generated by the repression of an activator, appears to facilitate response to unpredictability (noise) in extracellular DNA concentrations. These data show that the physiological response of competence at the population level can be predicted from the specific interactions comprising the negative feedback loop of the *B. subtilis* competence circuit.

The architectures of the native and synthetic circuits display distinct noise profiles. In particular, native and SynEx circuit architectures seem to have different optimal functional regimes for competence. While the native circuit can function optimally in the high-noise regime, the SynEx circuit can only do so in the low-noise regime. Lowering variability in native competence durations is possible by changing ComS parameter values (WeakS); however, these perturbations come at a cost of reduced competence durations and absolute transformation efficiency. Similarly, as the SynEx circuit approaches high variability in competence durations comparable to those observed in the native circuit, successful competence events become rare. Together, these results show that although parameterization is important, circuit architecture is also critical and can define the operational limits for genetic circuits. Numerous groups have studied this problem and compared parameterization versus circuit architecture and showed that certain properties of biological networks can only be accounted for by topology and not parameterization (Igoshin et al., 2007; Klemm and Bornholdt, 2005; Kollmann et al., 2005; Savageau, 2001; Tsai et al., 2008; Wall et al., 2003). For example, feed-forward loop motifs in transcriptional networks can have different architectures that appear to provide unique functional attributes that are independent of

parameterization (Dekel et al., 2005; Mangan and Alon, 2003). Similarly, native and SynEx circuit architectures have distinct limits for competence dynamics. Changing parameters only permits sampling of behaviors within these limits and therefore cannot account completely for properties dictated by circuit architecture.

Numerous genetic circuits contain multistep regulation pathways involving successive steps of activation and repression. Therefore, a comparative analysis of native and synthetic circuits that exhibit the same global mode of regulation, but with opposite order of reactions, represents a general approach to identify the functional importance of gene circuit architectures. This method could be applied to other biological systems to reveal why a given circuit architecture may have been selected over other, seemingly equivalent alternatives to regulate a specific physiological function. In particular, the finding that circuit architecture determines stochastic behavior, which in turn dictates the system's physiological response range, demonstrates that stochastic fluctuations can reveal the relationship between gene circuit architecture, dynamics, and function.

Depending on biological requirements and constraints, either the native or SynEx circuit architecture may be advantageous in terms of fitness (Figure 6C). It is, for example, interesting to note that the SynEx circuit, which exhibits precise dynamics, shares similar topology with genetic oscillators such as circadian-clock and cell-cycle circuits (see Figure S17), for which precision is known to be crucial for function (Bell-Pedersen et al., 2005; Liu et al., 1997; Mihalcescu et al., 2004; Pomerening et al., 2005; Rust et al., 2007; Yamaguchi et al., 2003). The reduced noise observed in SynEx and SynExSlow circuits may thus represent a fundamental circuit-level property and provide a possible explanation as to why genetic oscillators share a common circuit architecture. On the other hand, noisy operation of native competence circuit dynamics appears to be advantageous under unpredictable environmental conditions. Naturally occurring differences in extracellular DNA concentrations may thus have favored the particular negative feedback loop architecture of the native competence circuit. This suggests that topological variations of functionally analogous genetic circuits may be subject to evolutionary selection based on their noise characteristics.

EXPERIMENTAL PROCEDURES

Basic Strain Construction
The *Bacillus subtilis* strains used in this study are listed in Table S5. All strains are isogenic to wild-type *B. subtilis* PY79 strain. Strains were constructed with the following three chromosomal integration vectors: (1) pSac-Cm, which integrates into the *sacA* locus (constructed by R. Middleton and obtained from the Bacillus Genetic Stock Center), (2) pGlt-Kan, designed to integrate into the *gltA* locus (constructed by R. Middleton and obtained from the Bacillus Genetic Stock Center), and (3) pDR111, containing an IPTG-inducible promoter (pHyperspank) that integrates into *amyE* gene (kind gift from David Rudner, Harvard Medical School).

Transformation of *Bacillus subtilis* Strains
Bacillus subtilis strains were streaked on a Luria-Bertani (LB) broth agar plate and incubated overnight at 37°C with appropriate antibiotics. Cells from a single colony were inoculated in 10 ml of glucose minimal medium (Jarmer et al., 2002) with glutamate as the sole nitrogen source. The culture was grown at 37°C in a 25 ml flask with good aeration to an optical density (OD600) of ~0.8. 1 ml of this culture cells was incubated with the integrative expression plasmid pDP151-P_{rpsD}-*yfp* (described in the Supplemental Experimental Procedures [S2.7]) at 37°C for 40 min. Positive transformants were scored for erythromycin (Erm) resistance and constitutive *yfp* expression upon integration into the *thrC* locus.

Growth and Imagining Conditions
Bacillus subtilis cells were grown in LB at 37°C. Antibiotics for selection were added to the following final concentrations: 5 μg/ml chloramphenicol, 5 μg /ml neomycin, 10 μg/ml spectinomycin, and 5 μg/ml erythromycin. When necessary, the cultures were adjusted to the final IPTG concentrations of 20 μM and 2% Conditioned Media (CM) (described in the Supplemental Experimental Procedures [S2.8.1]).

Cells were grown at 37°C in LB to an optical density of 1.8 and resuspended in 0.5 volume of Resuspension Media (RM; composition [per 1 liter] 0.046 mg $FeCl_2$, 4.8 g $MgSO_4$, 12.6 mg $MnCl_2$, 535 mg NH_4Cl, 106 mg Na_2SO_4, 68 mg KH_2PO_4, 96.5 mg NH_4NO_3, 219 mg $CaCl_2$, 2 g L-glutamic acid) supplemented with 20 μM IPTG. After 1.5 hr incubation at 37°C, cells were diluted 10-fold in RM and applied onto a 1.5% low-melting agarose pad made with RM supplemented with 20 μM IPTG and 2% CM. This protocol is optimized for time-lapse microscopy.

Time-Lapse Microscopy
Growth of microcolonies was observed with fluorescence time-lapse microscopy at 37°C with an Olympus IX-81 inverted microscope with a motorized stage (ASI) and an incubation chamber. Image sets were acquired every 40 min with a Hamamatsu ORCA-ER camera. Custom Visual Basic software in combination with the Image Pro Plus (Media Cybernetics) was used to automate image acquisition and microscope control.

Image Analysis
Time-lapse movie data analysis were performed by custom software developed with MATLAB to analyze with the image processing and statistics toolboxes (TheMathworks) described in Rosenfeld et al. (2005) and Süel et al. (2006).

Mathematical Modeling
In order to predict the dynamical behavior of the native and SynEx circuit architectures, we derived continuous differential-equation models of the circuits using standard chemical kinetics rules. The models, described in detail in the Supplemental Data, account for the dynamical behavior of ComK and ComS/MecA concentrations. The dynamics of these models can be analyzed in the two-dimensional phase space formed by these two variables, (see Supplemental Experimental Procedures [S1.1.1 and S.1.2.1]). This phase-space analysis allowed us to determine the parameter ranges in which excitable behavior arises.

To introduce biochemical stochasticity in a realistic way, we wrote a set of biochemical reactions underlying the interactions of the two circuits (see the Supplemental Experimental Procedures [S.1.1.2]). We simulated those reactions by means of a Monte Carlo algorithm following Gillespie's method (Gillespie, 1977). The values of the reaction rates were chosen to match the deterministic parameters determined previously, and we checked that under those conditions the deterministic and stochastic descriptions were in agreement on average.

SUPPLEMENTAL DATA

Supplemental Data include Supplemental Experimental Procedures, 17 figures, and seven tables and can be found with this article online at http://www.cell.com/supplemental/S0092-8674(09)01033-2.

Cell

REFERENCES

Acar, M., Mettetal, J.T., and van Oudenaarden, A. (2008). Stochastic switching as a survival strategy in fluctuating environments. Nat. Genet. *40*, 471–475.

Alon, U. (2007). Network motifs: theory and experimental approaches. Nat. Rev. Genet. *8*, 450–461.

Bell-Pedersen, D., Cassone, V.M., Earnest, D.J., Golden, S.S., Hardin, P.E., Thomas, T.L., and Zoran, M.J. (2005). Circadian rhythms from multiple oscillators: lessons from diverse organisms. Nat. Rev. Genet. *6*, 544–556.

Berka, R.M., Hahn, J., Albano, M., Draskovic, I., Persuh, M., Cui, X., Sloma, A., Widner, W., and Dubnau, D. (2002). Microarray analysis of the Bacillus subtilis K-state: genome-wide expression changes dependent on ComK. Mol. Microbiol. *43*, 1331–1345.

Blake, W.J., Balazsi, G., Kohanski, M.A., Isaacs, F.J., Murphy, K.F., Kuang, Y., Cantor, C.R., Walt, D.R., and Collins, J.J. (2006). Phenotypic consequences of promoter-mediated transcriptional noise. Mol. Cell *24*, 853–865.

Dekel, E., Mangan, S., and Alon, U. (2005). Environmental selection of the feed-forward loop circuit in gene-regulation networks. Phys. Biol. *2*, 81–88.

Dubnau, D. (1999). DNA uptake in bacteria. Annu. Rev. Microbiol. *53*, 217–244.

Gillespie, D.T. (1977). Exact stochastic simulations of coupled chemical reactions. J. Phys. Chem. *81*, 2340.

Grossman, A.D. (1995). Genetic networks controlling the initiation of sporulation and the development of genetic competence in Bacillus subtilis. Annu. Rev. Genet. *29*, 477–508.

Hahn, J., Kong, L., and Dubnau, D. (1994). The regulation of competence transcription factor synthesis constitutes a critical control point in the regulation of competence in Bacillus subtilis. J. Bacteriol. *176*, 5753–5761.

Haijema, B.J., Hahn, J., Haynes, J., and Dubnau, D. (2001). A ComGA-dependent checkpoint limits growth during the escape from competence. Mol. Microbiol. *40*, 52–64.

Hamoen, L.W., Van Werkhoven, A.F., Bijlsma, J.J., Dubnau, D., and Venema, G. (1998). The competence transcription factor of Bacillus subtilis recognizes short A/T-rich sequences arranged in a unique, flexible pattern along the DNA helix. Genes Dev. *12*, 1539–1550.

Igoshin, O.A., Brody, M.S., Price, C.W., and Savageau, M.A. (2007). Distinctive topologies of partner-switching signaling networks correlate with their physiological roles. J. Mol. Biol. *369*, 1333–1352.

Jarmer, H., Berka, R., Knudsen, S., and Saxild, H.H. (2002). Transcriptome analysis documents induced competence of Bacillus subtilis during nitrogen limiting conditions. FEMS Microbiol. Lett. *206*, 197–200.

Klemm, K., and Bornholdt, S. (2005). Topology of biological networks and reliability of information processing. Proc. Natl. Acad. Sci. USA *102*, 18414–18419.

Kollmann, M., Lovdok, L., Bartholome, K., Timmer, J., and Sourjik, V. (2005). Design principles of a bacterial signalling network. Nature *438*, 504–507.

Kussell, E., and Leibler, S. (2005). Phenotypic diversity, population growth, and information in fluctuating environments. Science *309*, 2075–2078.

Liu, C., Weaver, D.R., Strogatz, S.H., and Reppert, S.M. (1997). Cellular construction of a circadian clock: period determination in the suprachiasmatic nuclei. Cell *91*, 855–860.

Maamar, H., and Dubnau, D. (2005). Bistability in the Bacillus subtilis K-state (competence) system requires a positive feedback loop. Mol. Microbiol. *56*, 615–624.

Maamar, H., Raj, A., and Dubnau, D. (2007). Noise in gene expression determines cell fate in Bacillus subtilis. Science *317*, 526–529.

Magnuson, R., Solomon, J., and Grossman, A.D. (1994). Biochemical and genetic characterization of a competence pheromone from B. subtilis. Cell *77*, 207–216.

Mangan, S., and Alon, U. (2003). Structure and function of the feed-forward loop network motif. Proc. Natl. Acad. Sci. USA *100*, 11980–11985.

Mihalcescu, I., Hsing, W., and Leibler, S. (2004). Resilient circadian oscillator revealed in individual cyanobacteria. Nature *430*, 81–85.

Ogura, M., Liu, L., Lacelle, M., Nakano, M.M., and Zuber, P. (1999). Mutational analysis of ComS: evidence for the interaction of ComS and MecA in the regulation of competence development in Bacillus subtilis. Mol. Microbiol. *32*, 799–812.

Pomerening, J.R., Kim, S.Y., and Ferrell, J.E., Jr. (2005). Systems-level dissection of the cell-cycle oscillator: bypassing positive feedback produces damped oscillations. Cell *122*, 565–578.

Quisel, J.D., Burkholder, W.F., and Grossman, A.D. (2001). In vivo effects of sporulation kinases on mutant Spo0A proteins in Bacillus subtilis. J. Bacteriol. *183*, 6573–6578.

Rosenfeld, N., Young, J.W., Alon, U., Swain, P.S., and Elowitz, M.B. (2005). Gene regulation at the single-cell level. Science *307*, 1962–1965.

Rust, M.J., Markson, J.S., Lane, W.S., Fisher, D.S., and O'Shea, E.K. (2007). Ordered phosphorylation governs oscillation of a three-protein circadian clock. Science *318*, 809–812.

Savageau, M.A. (2001). Design principles for elementary gene circuits: elements, methods, and examples. Chaos *11*, 142–159.

Smits, W.K., Eschevins, C.C., Susanna, K.A., Bron, S., Kuipers, O.P., and Hamoen, L.W. (2005). Stripping Bacillus: ComK auto-stimulation is responsible for the bistable response in competence development. Mol. Microbiol. *56*, 604–614.

Smits, W.K., Bongiorni, C., Veening, J.W., Hamoen, L.W., Kuipers, O.P., and Perego, M. (2007). Temporal separation of distinct differentiation pathways by a dual specificity Rap-Phr system in Bacillus subtilis. Mol. Microbiol. *65*, 103–120.

Stricker, J., Cookson, S., Bennett, M.R., Mather, W.H., Tsimring, L.S., and Hasty, J. (2008). A fast, robust and tunable synthetic gene oscillator. Nature *456*, 516–519.

Süel, G.M., Garcia-Ojalvo, J., Liberman, L.M., and Elowitz, M.B. (2006). An excitable gene regulatory circuit induces transient cellular differentiation. Nature *440*, 545–550.

Süel, G.M., Kulkarni, R.P., Dworkin, J., Garcia-Ojalvo, J., and Elowitz, M.B. (2007). Tunability and noise dependence in differentiation dynamics. Science *315*, 1716–1719.

Susanna, K.A., Mironczuk, A.M., Smits, W.K., Hamoen, L.W., and Kuipers, O.P. (2007). A single, specific thymine mutation in the ComK-binding site severely decreases binding and transcription activation by the competence transcription factor ComK of Bacillus subtilis. J. Bacteriol. *189*, 4718–4728.

Thattai, M., and van Oudenaarden, A. (2004). Stochastic gene expression in fluctuating environments. Genetics *167*, 523–530.

Tsai, T.Y., Choi, Y.S., Ma, W., Pomerening, J.R., Tang, C., and Ferrell, J.E., Jr. (2008). Robust, tunable biological oscillations from interlinked positive and negative feedback loops. Science *321*, 126–129.

Cell

Turcotte, M., Garcia-Ojalvo, J., and Süel, G.M. (2008). A genetic timer through noise-induced stabilization of an unstable state. Proc. Natl. Acad. Sci. USA *105*, 15732–15737.

Turgay, K., Hahn, J., Burghoorn, J., and Dubnau, D. (1998). Competence in Bacillus subtilis is controlled by regulated proteolysis of a transcription factor. EMBO J. *17*, 6730–6738.

van Sinderen, D., Luttinger, A., Kong, L., Dubnau, D., Venema, G., and Hamoen, L. (1995). comK encodes the competence transcription factor, the key regulatory protein for competence development in Bacillus subtilis. Mol. Microbiol. *15*, 455–462.

Wall, M.E., Hlavacek, W.S., and Savageau, M.A. (2003). Design principles for regulator gene expression in a repressible gene circuit. J. Mol. Biol. *332*, 861–876.

Wolf, D.M., Vazirani, V.V., and Arkin, A.P. (2005). Diversity in times of adversity: probabilistic strategies in microbial survival games. J. Theor. Biol. *234*, 227–253.

Yamaguchi, S., Isejima, H., Matsuo, T., Okura, R., Yagita, K., Kobayashi, M., and Okamura, H. (2003). Synchronization of cellular clocks in the suprachiasmatic nucleus. Science *302*, 1408–1412.